Triplet and beam interaction in a plasma

E. Peter, S. Marini, R. Pakter, and F. B. Rizzato

Citation: Physics of Plasmas **24**, 102124 (2017); doi: 10.1063/1.5005946
View online: https://doi.org/10.1063/1.5005946
View Table of Contents: http://aip.scitation.org/toc/php/24/10
Published by the American Institute of Physics

Triplet and beam interaction in a plasma

E. Peter,[a] S. Marini,[b] R. Pakter,[c] and F. B. Rizzato[d]
Instituto de Física, Universidade Federal do Rio Grande do Sul, Caixa Postal 15051, 91501-970 Porto Alegre, RS, Brazil

(Received 20 September 2017; accepted 2 October 2017; published online 19 October 2017)

The interaction of three waves requires wavelength and frequency matching conditions. Without the presence of a particle beam, if the conditions are satisfied and if the frequency of the envelope is lower than the lowest frequency of the waves, they exchange energy and the evolution of the envelope of each wave is given by a constant plus a sinusoidal function. On the other hand, if a particle beam propagates within electrostatic and electromagnetic fields with no wavelength and frequency match, the energy exchange between the modes is done due to the particles. One of the modes could be amplified in this scheme. In the present work, we propose a model where a non-relativistic particle beam propagates in a plasma within two electromagnetic modes and one electrostatic mode with wavelength and frequency matching conditions. Then, the waves are allowed to exchange energy between themselves and with the particle beam as well. We present new features in comparison to the isolated triplet interaction and to the beam-wave interaction. These features are relevant for a more realistic triplet interaction model. *Published by AIP Publishing.*
https://doi.org/10.1063/1.5005946

I. INTRODUCTION

The interaction of three waves, based on the wave triplet concept, is quite explored and accepted in the literature. In the analysis of a single triplet of waves, the interaction between the waves takes place when resonant conditions are established, i.e., the waves must satisfy frequency and wavelength matching conditions. This implies a relation like $\omega_1 = \omega_2 + \omega_3$ and $k_1 + k_2 = k_3$.[1–8] If the interaction parameter which is proportional to the plasma frequency is small enough, then the evolution of the envelope of the waves is well described by the modulational approximation—the dynamics of the envelope is regular and periodic.[9] Thus, the waves exchange energy, varying their amplitudes slowly, in a way that the total energy of the system is conserved, as seen in Ref. 2.

On the other hand, the interaction between waves and a charged particle beam in a plasma is already described in Ref. 14. In that work, the waves do not satisfy the frequency and wavelength matching conditions, and thus, the presence of the particle beam has a key role in the process: due—and only due—the beam, the waves could exchange energy in a conservative system. The authors included transversal and longitudinal modes, showing that the amplitudes of the longitudinal modes have a large growth. Usually, the growth occurs after a rearrangement time and it is exponential until saturation. An analogy is made in the present work between this behavior and the dynamics of a one-dimensional free-electron laser.[10–13]

In the present work, we allow the waves to interact with themselves based on the concept of the wave triplet and to interact with a non-relativistic particle beam in a plasma. The interaction between waves affects dramatically the system dynamics described in Ref. 14. We consider in this paper only three interacting modes propagating in a plasma: two transversal modes described by electromagnetic plane waves and one longitudinal mode vibrating with the plasma frequency. Here, we give a more realistic model for the triplet interaction, in the sense of including the interaction of resonant particles, which may be found immersed in the plasma. The whole scheme could also be applied, as discussed later, to amplify an electrostatic wave and to preserve some gain after a characteristic time. This feature is interesting, for example, to accelerate a second particle beam based on the physics of Ref. 15. Such as in Ref. 14, a fixed sinusoidal approximation is made for the wave fields.

This paper is organized as follows: in Sec. II, we introduce the basic physical model and the equations of motion; in Sec. III, we present the results in the absence of the particle beam; in Sec. IV, we effectively insert both the particle beam and the interaction between the waves in the system dynamics; and, finally, in Sec. V, we draw our conclusions.

II. PHYSICAL MODEL

In the present model, a non-relativistic charged particle beam propagates in a cold plasma interacting with one longitudinal and two transversal (a co-propagating and a counter-propagating) waves. The model proposed here is similar to the one given in Ref. 14. The main difference is that we also take into account the fluctuations of density ρ of the plasma. This allows the interaction between the wave modes even in the absence of the particle beam. The full Lagrangian that describes the model is written as

[a]peterpeter@uol.com.br
[b]marini@ufrgs.br
[c]pakter@if.ufrgs.br
[d]rizzato@if.ufrgs.br

$$L = \int d^3x \left[\frac{1}{2}mn|\vec{v}|^2 + \frac{1}{2}m\frac{\rho}{e}|\vec{v}|^2\right] + \frac{1}{8\pi}\int d^3x \left(\left|\nabla\Phi + \frac{1}{c}\frac{\partial\vec{A}}{\partial t}\right|^2 - |\vec{\nabla}\times\vec{A}|^2\right) + \int d^3x\left(\frac{1}{c}\vec{j}\cdot\vec{A} - \rho\Phi\right) + \sum_{i=1}^{N}\left[\frac{1}{2}m|\dot{\vec{r}}_i|^2 + e\Phi(\vec{r}_i,t) - \frac{e}{c}\dot{\vec{r}}_i\cdot\vec{A}(\vec{r}_i,t)\right], \quad (1)$$

where $n = const.$ is the particle density of the background plasma, $\rho(\vec{r},t)$ is the local fluctuation of charge density of the background plasma, $\vec{v}(\vec{r},t)$ is the Eulerian velocity, $\Phi(\vec{r},t)$ is the scalar potential, $\vec{A}(\vec{r},t)$ is the total vector potential, $\vec{j}(\vec{r},t)$ is the current, m is the mass of the electron, $\vec{r}_i(t)$ and $\dot{\vec{r}}_i(t)$ are the position and the velocity of the i-particle of the beam, and e is the charge of the electron.

While the fields are described by

$$\begin{aligned}\Phi &= \phi(t)\cos[k_L x - \omega_L t - \beta(t)],\\ \vec{A}_1 &= a_1(t)\cos[-k_1 x + \omega_1 t - \theta_1(t)]\hat{\mathbf{e}},\\ \vec{A}_2 &= a_2(t)\cos[-k_2 x - \omega_2 t - \theta_2(t)]\hat{\mathbf{e}},\end{aligned} \quad (2)$$

where $\phi(t)$, $a_1(t)$, and $a_2(t)$ are the slowly varying amplitudes, $\beta(t)$, $\theta_1(t)$, and $\theta_2(t)$ are the slowly varying phases, $\omega_L = \omega_p$, $\vec{A} = \vec{A}_1 + \vec{A}_2$, $\hat{\mathbf{e}}$ is the polarization versor, $\omega_1 = \omega_2 + \omega_p$ is the frequency matching condition, and $\omega_p^2 = 4\pi ne^2/m$ is the plasma frequency. Moreover, the dispersion relation for the electromagnetic waves is described by $\omega_i^2 = \omega_p^2 + k_i^2c^2$. Finally, the wavelength relation between the waves is written as $k_L = k_1 + k_2$. If we consider $\omega_1 = \alpha\omega_p$, where $\alpha > 1$ is a given parameter, we get $\omega_2 = (\alpha - 1)\omega_p$, $k_1 = \omega_p\sqrt{\alpha^2-1}/c$, and $k_2 = \omega_p\sqrt{(\alpha-1)^2-1}/c$. This implies that the resonance velocity of the beam is given by $v_r = \omega_p/k_L = c/(\sqrt{\alpha^2-1} - \sqrt{(\alpha-1)^2-1})$. As we increase α, v_r becomes smaller. For example, for $\alpha = 5$, $v_r = 0.114c$, and for $\alpha = 20$, $v_r = 0.0257c$. We point out that $\vec{A}_2$ is a field of a counter-propagating wave.

Exactly as Ref. 14, we assume the following linear relations for the background plasma:

$$\begin{aligned}\vec{v}_\parallel &= \frac{1}{4\pi ne}\frac{\partial\nabla\Phi}{\partial t},\\ \vec{v}_\perp &= \frac{e}{mc}\vec{A},\\ \vec{j}_\parallel &= -en\vec{v}_\parallel,\\ \vec{j}_\perp &= -en\vec{v}_\perp,\\ \rho &= -\frac{1}{4\pi}\nabla^2\Phi,\end{aligned} \quad (3)$$

where $\vec{v}_\parallel$ and $\vec{v}_\perp$ are the longitudinal and transverse velocities.

Assuming periodic boundary conditions, we substitute Eqs. (2) and (3) into Eq. (1) and we average the Lagrangian over a box of size l. This way, we find

$$\begin{aligned}L = &\sum_{i=1}^{N}\frac{1}{2}m(\dot{x}_i^2 + \dot{y}_i^2) + e\sum_{i=1}^{N}\phi\cos(k_L x_i - \omega_p t - \beta)\\ &- \frac{e}{c}\sum_{i=1}^{N}\dot{y}_i[a_1\cos(-k_1 x_i + \omega_1 t - \theta_1)]\\ &- \frac{e}{c}\sum_{i=1}^{N}\dot{y}_i[a_2\cos(-k_2 x_i - \omega_2 t - \theta_2)]\\ &+ \frac{l^3\dot{\beta}}{8\pi\omega_p}\phi^2 + \frac{l^3}{8\pi c^2}\left(-\omega_1\dot{\theta}_1 a_1^2 + \omega_2\dot{\theta}_2 a_2^2\right)\\ &+ \frac{l^3 e}{32\pi mc^2}k_L^2\phi a_1 a_2\cos(-\beta - \theta_1 - \theta_2).\end{aligned} \quad (4)$$

Lagrangian of Eq. (4) is rewritten in terms of dimensionless variables

$$\begin{aligned}L = &\frac{1}{2}\left(\frac{2n_b}{n}\right)\left[\langle\dot{\xi}_i^2\rangle + \langle\dot{\eta}_i^2\rangle\right] + \left(\frac{2n_b}{n}\right)\sqrt{J}\langle\cos(\xi_i - \beta)\rangle\\ &- \left(\frac{2n_b}{n}\right)\sqrt{\frac{\omega_p I_1}{\omega_1\mu_1}}\langle\dot{\eta}_i\cos(\mu_1[\xi_i + \theta_1])\rangle\\ &+ \left(\frac{2n_b}{n}\right)\sqrt{\frac{\omega_p I_2}{\omega_2\mu_2}}\langle\dot{\eta}_i\cos(\mu_2[\xi_i + \theta_2])\rangle\\ &+ \dot{\beta}J + \left(1 - \frac{\omega_1}{\mu_1\omega_p} - \dot{\theta}_1\right)I_1 + \left(-1 - \frac{\omega_2}{\mu_2\omega_p} + \dot{\theta}_2\right)I_2\\ &+ \frac{1}{4}\sqrt{\frac{\omega_p^2 I_1 I_2 J}{\omega_1\omega_2\mu_1\mu_2}}\cos(\beta + \mu_1\theta_1 + \mu_2\theta_2),\end{aligned} \quad (5)$$

where

$$\begin{aligned}\xi_i &= k_L x_i - \omega_p t,\\ \eta_i &= k_L y_i,\\ t &= \omega_p t,\\ \phi^2 &= \left(\frac{m\omega_p^2}{ek_L^2}\right)^2 J,\\ a_j^2 &= \left(\frac{mc\omega_p}{ek_L}\right)^2\left(\frac{\omega_p}{\omega_j}\right)\frac{I_j}{\mu_j},\\ \mu_1\theta_1 &= \theta_1 + \mu_1\omega_p t - \omega_1 t,\\ \mu_2\theta_2 &= \theta_2 + \mu_2\omega_p t + \omega_2 t,\\ \mu_j &= \frac{k_j}{k_L},\\ n_b &= \frac{N}{l^3},\end{aligned} \quad (6)$$

and N is the number of particles. The brackets indicate a mean value over the beam particle distribution, i.e., $\langle x\rangle = \sum_{i=1}^{N} x_i/N$. Through the Lagrangian of Eq. (5), the equations of motion of the system are obtained and written as follows:

$$
\begin{aligned}
\ddot{\xi}_i &= -\sqrt{J}\sin(\xi_i-\beta)+\mu_1\sqrt{\frac{\omega_p I_1}{\omega_1\mu_1}}\dot{\eta}_i\sin(\mu_1[\xi_i+\theta_1])+\mu_2\sqrt{\frac{\omega_p I_2}{\omega_2\mu_2}}\dot{\eta}_i\sin(\mu_2[\xi_i+\theta_2]),\\
\ddot{\eta}_i &= \left(\frac{\omega_p}{\omega_1}\right)^{\frac{1}{2}}\sqrt{\frac{I_1}{\mu_1}}\frac{\dot{I}_1}{2I_1}\cos[\mu_1(\xi_i+\theta_1)]-\left(\frac{\omega_p}{\omega_1}\right)^{\frac{1}{2}}\sqrt{\frac{I_1}{\mu_1}}\mu_1(\dot{\xi}_i+\dot{\theta}_1)\sin[\mu_1(\xi_i+\theta_1)]\left(\frac{\omega_p}{\omega_2}\right)^{\frac{1}{2}}\sqrt{\frac{I_2}{\mu_2}}\frac{\dot{I}_2}{2I_2}\cos[\mu_2(\xi_i+\theta_2)]\\
&\quad-\left(\frac{\omega_p}{\omega_2}\right)^{\frac{1}{2}}\sqrt{\frac{I_2}{\mu_2}}\mu_2(\dot{\xi}_i+\dot{\theta}_2)\sin[\mu_2(\xi_i+\theta_2)],\\
\dot{\beta} &= -\frac{1}{8}\sqrt{\frac{\omega_p^2 I_1 I_2}{\omega_1\omega_2\mu_1\mu_2 J}}\cos(\beta+\mu_1\theta_1+\mu_2\theta_2)-\frac{1}{2}\left(\frac{2n_b}{n}\right)J^{-1/2}\langle\cos(\xi_i-\beta)\rangle,\\
\dot{J} &= -\frac{1}{4}\sqrt{\frac{\omega_p^2 I_1 I_2 J}{\omega_1\omega_2\mu_1\mu_2}}\sin(\beta+\mu_1\theta_1+\mu_2\theta_2)+\left(\frac{2n_b}{n}\right)J^{1/2}\langle\sin(\xi_i-\beta)\rangle,\\
\dot{\theta}_1 &= 1-\frac{\omega_1}{\mu_1\omega_p}+\frac{1}{8}\sqrt{\frac{\omega_p^2 I_2 J}{\omega_1\omega_2\mu_1\mu_2 I_1}}\cos(\beta+\mu_1\theta_1+\mu_2\theta_2)-\frac{1}{2}\left(\frac{2n_b}{n}\right)\sqrt{\frac{\omega_p}{\omega_1\mu_1 I_1}}\langle\dot{\eta}_i\cos(\mu_1[\xi_i+\theta_1])\rangle,\\
\dot{I}_1 &= \frac{\mu_1}{4}\sqrt{\frac{\omega_p^2 I_1 I_2 J}{\omega_1\omega_2\mu_1\mu_2}}\sin(\beta+\mu_1\theta_1+\mu_2\theta_2)-\left(\frac{2n_b}{n}\right)\mu_1\sqrt{\frac{\omega_p I_1}{\omega_1\mu_1}}\langle\dot{\eta}_i\sin(\mu_1[\xi_i+\theta_1])\rangle,\\
\dot{\theta}_2 &= 1+\frac{\omega_2}{\mu_2\omega_p}-\frac{1}{8}\sqrt{\frac{\omega_p^2 I_1 J}{\omega_1\omega_2\mu_1\mu_2 I_2}}\cos(\beta+\mu_1\theta_1+\mu_2\theta_2)+\frac{1}{2}\left(\frac{2n_b}{n}\right)\sqrt{\frac{\omega_p}{\omega_2\mu_2 I_2}}\langle\dot{\eta}_i\cos(\mu_2[\xi_i+\theta_2])\rangle,\\
\dot{I}_2 &= -\frac{\mu_2}{4}\sqrt{\frac{\omega_p^2 I_1 I_2 J}{\omega_1\omega_2\mu_1\mu_2}}\sin(\beta+\mu_1\theta_1+\mu_2\theta_2)+\left(\frac{2n_b}{n}\right)\mu_2\sqrt{\frac{\omega_p I_2}{\omega_2\mu_2}}\langle\dot{\eta}_i\sin(\mu_2[\xi_i+\theta_2])\rangle,
\end{aligned}
\tag{7}
$$

where $\dot{\xi}_i$ is the longitudinal velocity in the longitudinal wave frame and $\dot{\eta}_i$ is the transverse velocity of the ith particle. These equations completely describe the model.

III. THREE WAVE INTERACTION

In this section, the case of the three wave interaction is briefly discussed, neglecting the presence of the particle beam, which corresponds to $n_b = 0$.

As can be seen in the equations of motion [Eq. (8)] below obtained from the normalized Lagrangian [Eq. (5)] in the particle beam absence, the Manley-Rowe relations[16] can be found: $I_1/\mu_1 + I_2/\mu_2 = c_1$, $I_1/\mu_1 + J = c_2$, and $J - I_2/\mu_2 = c_3$, where c_i are constants. The power flow of the waves $\omega_1 I_1/\mu_1 + \omega_2 I_2/\mu_2 + \omega_p J = c_4$ is also conserved. Thus, the waves exchange energy in a periodic fashion in this case. This behavior is expected for a wave triplet interaction[2] considering the modulational approximation, where the frequency of the envelope is much smaller than the high frequency of each wave. The regular behavior could be destroyed if we allowed the system to have sufficiently high intensities for the waves and a frequency mismatch $\Omega \neq 0$, where $\Omega = \omega_1 - \omega_2 - \omega_p \ll \omega_p$ or if we included an extra mode in the system.[4,5,7,17] In the present analysis, we always consider the perfectly matched case with $\Omega = 0$,

$$
\begin{aligned}
\dot{\beta} &= -\frac{1}{8}\sqrt{\frac{\omega_p^2 I_1 I_2}{\omega_1\omega_2\mu_1\mu_2 J}}\cos(\beta+\mu_1\theta_1+\mu_2\theta_2),\\
\dot{J} &= -\frac{1}{4}\sqrt{\frac{\omega_p^2 I_1 I_2 J}{\omega_1\omega_2\mu_1\mu_2}}\sin(\beta+\mu_1\theta_1+\mu_2\theta_2),\\
\dot{\theta}_1 &= 1-\frac{\omega_1}{\mu_1\omega_p}+\frac{1}{8}\sqrt{\frac{\omega_p^2 I_2 J}{\omega_1\omega_2\mu_1\mu_2 I_1}}\cos(\beta+\mu_1\theta_1+\mu_2\theta_2),\\
\dot{I}_1 &= \frac{\mu_1}{4}\sqrt{\frac{\omega_p^2 I_1 I_2 J}{\omega_1\omega_2\mu_1\mu_2}}\sin(\beta+\mu_1\theta_1+\mu_2\theta_2),\\
\dot{\theta}_2 &= 1+\frac{\omega_2}{\mu_2\omega_p}-\frac{1}{8}\sqrt{\frac{\omega_p^2 I_1 J}{\omega_1\omega_2\mu_1\mu_2 I_2}}\cos(\beta+\mu_1\theta_1+\mu_2\theta_2),\\
\dot{I}_2 &= -\frac{\mu_2}{4}\sqrt{\frac{\omega_p^2 I_1 I_2 J}{\omega_1\omega_2\mu_1\mu_2}}\sin(\beta+\mu_1\theta_1+\mu_2\theta_2).
\end{aligned}
\tag{8}
$$

In Fig. 1, we show the evolution of the envelope of the waves for $\omega_1 = 20$, $\omega_p = 1$, $J(t=0) = 10^{-4}$, $I_1(t=0) = I_2(t=0) = 2$, and $\beta(t=0) = \theta_1(t=0) = \theta_2(t=0) = 0$. As can be seen in this figure, while I_1, denoted by the solid black line, which has the higher frequency, grows (decays), I_2, solid blue line, and J, solid green line, decay (grow). It is a consequence of power flow conservation. The envelope of the waves oscillates with the same frequency, independently of the wave. We call this frequency the frequency of the envelope ω_{3W}.

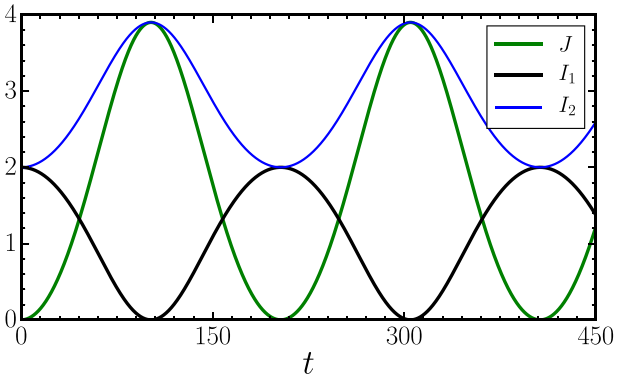

FIG. 1. In green, the evolution of J, while in black, the evolution of I_1 and in blue, the evolution of I_2. The figure was built for $\omega_1 = 20, \omega_p = 1, J(t=0) = 10^{-4}, I_1(t=0) = I_2(t=0) = 2, \beta(t=0) = \theta_1(t=0) = \theta_2\ (t=0) = 0$.

The frequency of the envelope (ω_{3W}) depends on the total energy of the system and on the plasma frequency. As we increase ω_p, ω_{3W} also increases. In Fig. 2, we plot a map where in the vertical axis is expressed ω_p, in the horizontal axis is expressed t, and the colors represent the value of J. Thus, the map is the time evolution of J for different ω_p. To build the map, we kept $c_4 = 156$, $\omega_1 = 20$, $I_1(t=0) = 2$, and $I_2(t=0) = 2$ constant and we varied ω_p (and, consequently, ω_2). The frequency of the envelope grows as ω_p increases, as shown by the compression of the curves. The phase-velocity of J ($v_0 = \omega_p/k_L$, which is, in fact, identical to v_r) varies from almost zero (for $\omega_p \approx 0$) to $0.4c$, in the case of $\omega_p \approx 9.5$.

To complete the map of Fig. 2, in Fig. 3, explicitly, the frequency of the envelope (ω_{3W}) against the plasma frequency is shown. The frequency of the envelope grows linearly for small values of the plasma frequency. Even for $\omega_p = 8$, for example, ω_{3W} is much smaller than ω_p. This condition is necessary for the modulation approximation used in this paper.

Although the amplitude of J could grow, due to the regular and periodic dynamics of the envelope, the growth is not maintained along the time. Thus, this kind of system is not indicated, for example, to amplify the longitudinal mode. We point out that we could work with higher intensities for the waves and a frequency mismatch together, in order to break the regular behavior of the triplet interaction. Additional modes could be included as well.[4,8,18]

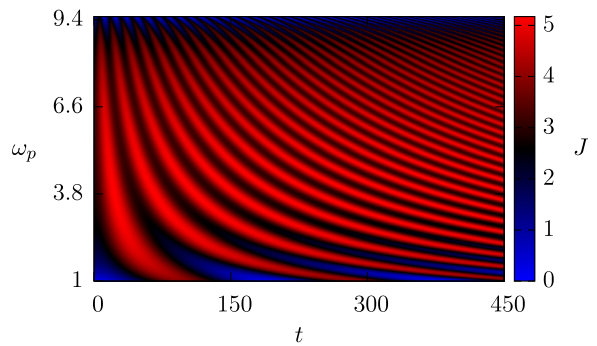

FIG. 2. Map of the evolution of J for different values of the plasma frequency ω_p, maintaining fixed $c_4 = 156$ and $\omega_1 = 20$, $I_1(t=0) = I_2(t=0) = 2$. Then, $J(t=0) = c_4/\omega_p - (\omega_1 I_1/\mu_1 + \omega_2 I_2/\mu_2)/\omega_p$.

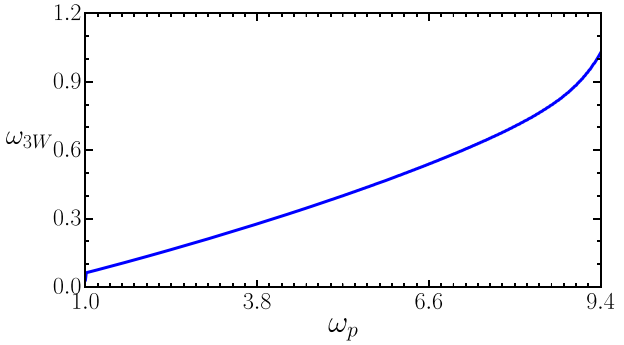

FIG. 3. Frequency of the envelope ω_{3W} vs. plasma frequency ω_p, maintaining fixed $c_4 = 156, \omega_1 = 20, I_1\ (t=0) = I_2(t=0) = 2$.

IV. FULL MODEL

In this section, the full model is explored. The results are shown turning on and off the triplet interaction and the particle-wave interaction.

As in Ref. 14, if we do not take into account the interaction between the waves, starting with a very small initial value of J, after a rearrangement time, J grows exponentially almost until it saturates. The exponential growth ceases when the mixing process takes place in the phase-space of the particles (it occurs when the particle distribution in this space becomes a non-single valued function). After the onset of the mixing process, the amplitude of J reaches the maximum value and then oscillates.

The whole dynamics is similar to what happens in a one-dimensional single pass free-electron laser: a FEL is a device that could efficiently convert the kinetic energy from a relativistic electron beam into electromagnetic energy in the form of radiation. To make this possible, the beam and the electromagnetic wave to be amplified (the laser or radiation) propagate in a spatially periodic and time-independent magnetic field produced by a wiggler. The combined action of the wiggler and laser fields forms the ponderomotive potential, which is responsible for the energy conversion.[10–13,19] In the FEL case, the evolution of the laser field occurs as the evolution of J, a rearrangement time, then an exponential growth, the first peak and oscillations with frequency in the order of the plasma frequency. The turning point from linear growth to saturation is also related to the onset of the mixing process. Moreover, the initial velocity that maximizes the growth rate of the amplified mode is slightly greater than the resonance velocity (the difference of velocities is related to the detuning[11–13,19]) and if the beam has an initial distribution of velocities, just as in FEL, the growth rate becomes smaller.[12,13]

While in the FEL dynamics, the laser field[10]—a transversal plane wave—is amplified, in this case, the longitudinal mode is amplified J. One of the reasons for that is because in the present model, the beam velocity is limited to non-relativistic velocities. This implies that the coupling between transversal fields and particles is weak. All of the features discussed here are presented through the evolution of J, denoted by the blue solid line, in Fig. 4, for $n_b/n = 0.1$, $\omega_1 = 20$, $\omega_p = 1$, $v_0 = \omega_p/k_L$, $\dot{\xi}(t=0) = 0$, $I_1(t=0) = 2$, $I_2(t=0) = 2$, and $J(t=0) = 10^{-4}$.

The green solid line in Fig. 4 shows the evolution of the system in the absence of the particle beam. As we show in Sec. III, in this case, the three waves exchange energy in a way that J has a regular and periodic behavior, oscillating along the time. The period of oscillations is about $T = 200$.

The black solid line represents the evolution of the amplitude of J in the presence of the particle beam and turning on the triplet interaction. Some features must be pointed out: there is no rearrangement time in the beginning of the motion because the system is initially driven by the triplet interaction, as can be seen in panel (a) of Fig. 4; the dynamics of the amplitude has two characteristic frequencies—the lowest one is related to the triplet frequency, while the highest one is related to the plasma frequency; the amplitude of J never goes back to its initial value due the presence of the beam particle; the mean-value of J is greater in the case of the full system in comparison to the value obtained turning off the triplet interaction. In fact, the largest peak value of J is achieved when the beam is not taken into account. However, this scenario may be seen as less realistic in the sense that it completely disregards the presence of resonant electrons immersed in the plasma.

In Figs. 5(a) and 5(b), the evolution of the electromagnetic modes I_1 and I_2 is plotted, using the same parameters as in Fig. 4. The blue solid lines represent the evolution of I_1 and I_2 without the wave interaction, the green solid lines represent that in the absence of the particle beam, and finally, the black solid lines for the full model. As can be seen, there is no significant change in these amplitudes in the case without the wave interaction. In the absence of the particle beam, the amplitudes of I_1 and I_2 vary significantly. The reason why is explained taking the initial values of I_1, I_2, and J and the Manley-Rowe relations $[I_1(t=0)/\mu_1 \approx I_2(t=0)/\mu_2 \gg J(t=0)]$. In the full model, an intermediate behavior is shown.

In terms of application, we may think in a system composed of the present scheme and a second particle beam. The initial velocity of the second beam is relativistic and does not have any kind of resonance with the quantities shown during this work. This way, the second beam only interacts with the waves and there is no ponderomotive potential effect acting over the beam. In Ref. 15, the envelope of the electrostatic mode has a Gaussian shape. Differently, here the envelope of J grows exponentially and reaches saturation. Besides that, the same physical principle of Ref. 15 could be used to accelerate the second particle beam. We point out that, due the oscillations of J after the saturation, the velocity of the second particle beam also oscillates, but even with the oscillations, the net gain could be appreciable—the oscillations of the velocity are not expressive in Ref. 15 because of the shape of the electrostatic field.

In Fig. 6, the phase-space $\dot{x}\ vs.\ \xi$ for different situations is shown. Panels (a), (b), and (c) show the initial phase-space configuration, the phase-space at the beginning of the onset of the mixing process. and a picture of the phase-space after the onset of the mixing process, respectively, for the full model. Panels (d), (e), and (f) were built for the case of no triplet interaction. Panel (d) shows the initial phase-space configuration, while (e) is a picture of the phase-space at the beginning of the onset of the mixing process and (f) is a

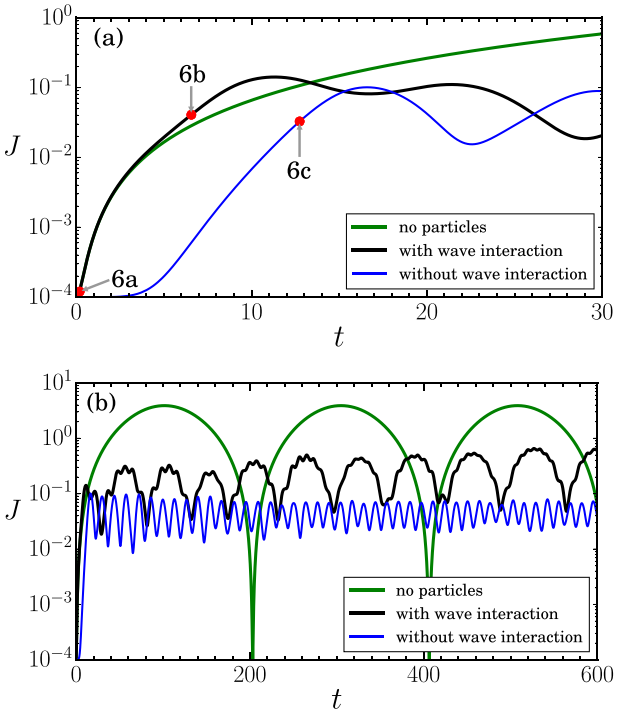

FIG. 4. Longitudinal mode evolution using the following parameters: $n_b/n = 0.1$, $\omega_1 = 20$, $\omega_p = 1$, $\dot{\xi}(t=0) = 0$ and the following initial conditions $I_1(t=0) = 2$, $I_2(t=0) = 2$ and $J(t=0) = 10^{-4}$, $\beta(t=0) = \theta_1(t=0) = \theta_2(t=0) = 0$. The points 6b and 6e represent when the mixing process starts for the full model and for the case one neglects the triplet interaction, respectively. Panel (a) is a zoom of panel (b), showing, in detail, the beginning of the dynamics.

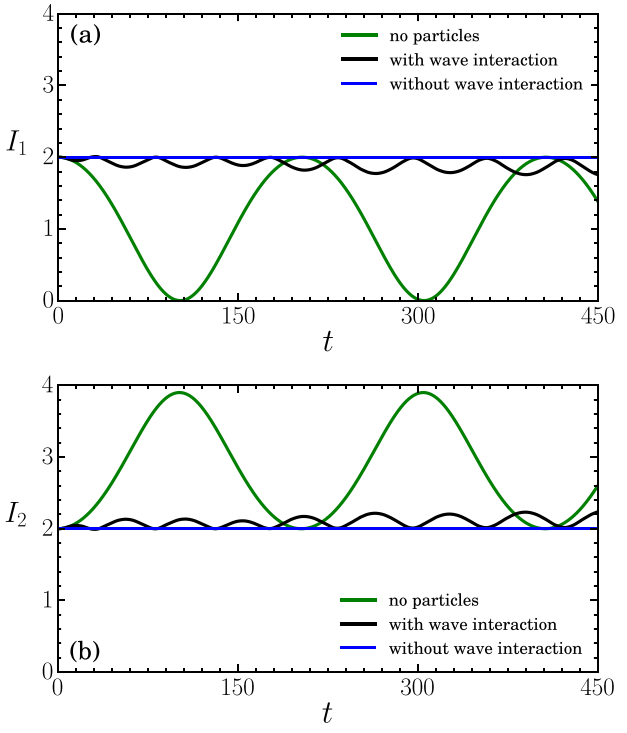

FIG. 5. Electromagnetic mode evolution for I_1 in panel (a) and for I_2 in panel (b), using the following parameters: $n_b/n = 0.1$, $\omega_1 = 20$, $\omega_p = 1$, $\dot{\xi}(t=0) = 0$ and the following initial conditions $I_1(t=0) = 2$, $I_2(t=0) = 2$ and $J(t=0) = 10^{-4}$, $\beta(t=0) = \theta_1(t=0) = \theta_2(t=0) = 0$.

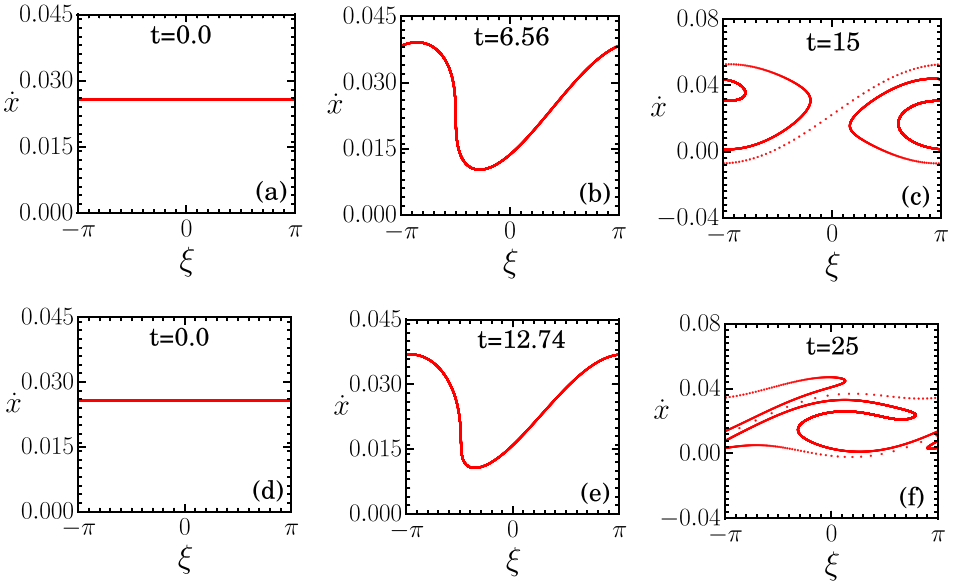

FIG. 6. Phase space snapshot for different situations. Panels (a), (b), and (c) are for the full model, while (d), (e), and (f) are from turning off the triplet interaction. The phase space configuration when simulations start are shown in panels (a) t = 0 and (d) t = 0. The phase space configuration at the onset of the mixing process is shown in panels (b) t = 6.56 and (e) t = 12.74, while the configuration after the onset of the mixing process is shown in panels (c) t = 15 and (f) t = 25.

snapshot after the onset. Typically, the onset of the mixing process occurs earlier in the full model: the triplet interaction speeds up the exchange of the energy process between the modes, eliminating the rearrangement time. The value of J at the onset of the mixing process is greater for the full model, but the peak value comes closer as the relation n_b/n is increased.

In Fig. 7, the value of the amplitude J at the onset of the mixing process ($J(t = t_{os})$) vs. n_b/n is shown. As can be seen, when the beam density is increased, the value of $J(t_{os})$ is also increased. It occurs because there are more particles to transfer the energy between the modes. In the case without the wave interaction, denoted by the red solid line, for $n_b/n < 0.15$, $J(t_{os})$ is smaller than in the full model (dashed blue line) because the dynamics is mainly driven by the triplet interaction. As we increase n_b/n, we offer more particles and consequently more energy to the system. However, the triplet interaction anticipates the onset of the mixing, so, we see that for $n_b/n > 0.15$, the value of J evaluated at the onset of the mixing process is greater in the case without the wave interaction.

Moreover, an increase in n_b/n reduces the time until the onset of the mixing process. As in Ref. 14, the relation n_b/n is limited to the order of 0.4 due to the sinusoidal approximation of the electrostatic wave. Higher values of n_b/n could change the shape of this mode.

V. CONCLUSIONS

We have investigated the interaction of a triplet and a particle beam in a plasma. In the proposed model, if we neglect the particle beam, the interaction between two transversal modes and a longitudinal mode (these modes satisfy the wavelength and frequency matching conditions) produces a regular and periodic behavior to the envelope of the waves. The frequency of the envelope depends on the total energy of the system and on the plasma frequency. In order to avoid chaos, we took parameters such as the frequency of the envelope is much smaller than the plasma frequency.[2]

On the other hand, if we ignore the direct interaction between the waves, the longitudinal mode J grows exponentially after a rearrangement time.[14] The growth ceases just after the onset of a mixing process in the phase space (the distribution function becomes a non-single valued function), J reaches the saturation, and then it oscillates around a mean value with a frequency comparable to the plasma frequency. The whole process is similar to what happens in a FEL.[10–13,19]

When we turn on both the triplet and the plasma beam interaction, the final result is a combination of the effects of these two interactions. In a real plasma, particles are immersed in the plasma in a way that resonant particles could exchange energy with the three waves, changing the triplet dynamics, even for a low density of resonant particles. Usually, in the present model, the J envelope is initially driven by the triplet, so there is no rearrangement time. Then, J grows exponentially and reaches the saturation just after the onset of the mixing process. Instead of returning to its initial value, the J dynamics has two characteristic frequencies (the lowest one is related to the triplet frequency, while the highest one is related to the plasma frequency) and its value oscillates near the peak of the amplitude. Moreover, the peak value of J is greater than

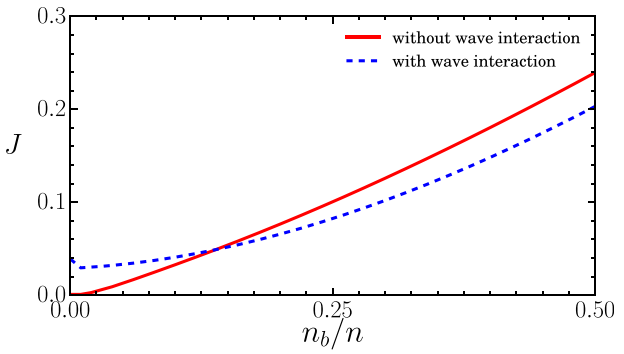

FIG. 7. Value of the amplitude J evaluated at the onset of the mixing process ($t = t_{os}$) as a function of n_b/n for the full model (dashed blue line) and for the case one neglects the triplet interaction (solid red line). The figure was built using the following initial conditions $I_1(t = 0) = I_2(t = 0) = 2$ and $J(t = 0) = 10^{-4}$, $\dot{\xi}(t = 0) = 0$, and $\beta(t = 0) = \theta_1(t = 0) = \theta_2(t = 0) = 0$.

the case in which we consider the presence of the particle beam and we ignore the triplet interaction.

The main conclusion in this paper is that the presence of a particle beam modifies the triplet dynamics even for a low density of particles. Thus, a more realistic triplet interaction model must include the interaction with the particles of the plasma. Moreover, frequency and wavelength matching conditions could be explored, when it is possible, to extract the maximum performance in low density particle beam and wave interactions in order to amplify the longitudinal mode and to produce a gain sustained along the time.

Despite the complexity of the presented model, velocities are restricted to non-relativistic values, for example. A relativistic model based on the relativistic model based on Ref. 20 must be developed. In addition, the shape of the longitudinal mode could be significantly changed due to the particle distribution if we increase the particle density of the beam. Beyond that, chaos could be also introduced by allowing a frequency mismatch between the waves and adding new modes in the system.[4–6,8,18,21,22] The chaos could be interesting in the point of view of J amplification. These topics should be explored in upcoming papers in order to provide a more accurate model.

ACKNOWLEDGMENTS

This work was supported by CAPES, CNPq, and FAPERGS, Brazil, and by the Air Force Office of Scientific Research (AFOSR), USA, under the Grant No. FA9550-16-1-0280.

[1]S. G. Thornhill and D. ter Haar, Phys. Rep. **43**, 43 (1978).
[2]P. Iorra, S. Marini, E. Peter, R. Pakter, and F. B. Rizzato, Physica A **436**, 686 (2015).
[3]F. B. Rizzato and A. C.-L. Chian, J. Plasma Phys. **48**, 71 (1992).
[4]P. M. Drysdale and P. A. Robinson, Phys. Plasmas **9**, 4896 (2002).
[5]M. Frichembruder, R. Pakter, G. Gerhardt, and F. B. Rizzato, Phys. Rev. E **62**, 7861 (2000).
[6]G. I. de Oliveira, L. P. L. de Oliveira, and F. B. Rizzato, Physica D **104**, 119 (1997).
[7]G. I. de Oliveira, M. Frichembruder, and F. B. Rizzato, Physica D **164**, 59 (2002).
[8]E. Peter, S. Marini, A. T. Chávez, and F. B. Rizzato, Physica A **463**, 103 (2016).
[9]A. M. Batista, I. L. Caldas, S. R. Lopes, R. L. Viana, W. Horton, and P. J. Morrison, Phys. Plasmas **13**, 042510 (2006).
[10]R. Bonifacio, F. Casagrande, G. Cerchioni, L. de Salvo Souza, P. Pierini, and N. Piovella, Riv. Nuovo Cimento **13**, 1 (1990).
[11]E. Peter, A. Endler, F. B. Rizzato, and A. Serbeto, Phys. Plasmas **20**, 123104 (2013).
[12]E. Peter, A. Endler, and F. B. Rizzato, Phys. Plasmas **21**, 113104 (2014).
[13]E. Peter, F. B. Rizzato, and A. Endler, J. Plasma Phys. **82**, 905820307 (2016).
[14]E. G. Evstatiev, W. Horton, and P. J. Morrison, Phys. Plasmas **10**, 4090 (2003).
[15]S. Marini, E. Peter, G. I. de Oliveira, and F. B. Rizzato, Phys. Plasmas **24**, 093113 (2017).
[16]J. M. Manley and H. E. Rowe, Proc. IRE **44**, 304 (1956).
[17]A. C.-L. Chian, S. R. Lopes, and J. R. Abalde, Physica D **99**, 269 (1996).
[18]R. Pakter, S. R. Lopes, and R. L. Viana, Physica D **110**, 277 (1997).
[19]E. Peter, F. B. Rizzato, and A. Endler, J. Plasma Phys. **83**, 905830302 (2017).
[20]E. G. Evstatiev, P. J. Morrison, and W. Horton, Phys. Plasmas **12**, 072108 (2005).
[21]F. B. Rizzato, R. Pakter, and S. R. Lopes, Phys. Rev. E **68**, 056601 (2003).
[22]M. Frichembruder, R. Pakter, and F. B. Rizzato, J. Plasma Phys. **71**, 11 (2005).